

## Non-coplanar ( $p, p\alpha$ ) and ( $p, d^3\text{He}$ ) reactions on ${}^9\text{Be}$ at 101.5 MeV

A. Nadasen, N. S. Chant, P. G. Roos, T. A. Carey,\* R. Cowen, C. Samanta, and J. Wesick

*Department of Physics and Astronomy, University of Maryland, College Park, Maryland 20742*

(Received 25 April 1980)

The ( $p, p\alpha$ ) and ( $p, d^3\text{He}$ ) reactions on  ${}^9\text{Be}$  have been investigated at a bombarding energy of 101.5 MeV in a non-coplanar geometry. Coincident data were obtained for coplanar angles  $\theta_{p,d} = 81.2^\circ$  and  $\theta_{\alpha,{}^3\text{He}} = -41.0^\circ$ , and the  $\alpha({}^3\text{He})$  detector ranging from  $\beta = 0^\circ$  to  $20^\circ$  out of the plane. These data show a smooth reduction in cross section with increasing  $\beta$ . Comparisons with distorted-wave impulse approximation calculations show that the reactions are dominated by quasifree processes, and that the  $D$ -state component of the  ${}^9\text{Be}$  wave function dominates for large  $\beta$ . Absolute spectroscopic factors for the  $S$ - and  $D$ -state terms extracted from the two different reactions are consistent and in excellent agreement with theoretical predictions.

NUCLEAR REACTIONS  ${}^9\text{Be}(p, p\alpha)$  and  ${}^9\text{Be}(p, d^3\text{He})$ ,  $E_{\text{lab}} = 101.5$  MeV; measured  $d^3\sigma/d\Omega_1 d\Omega_2 dE_1(E_1, E_2, \theta_1, \theta_2, \beta_2)$ ; Non-coplanar geometry; DWIA analysis; deduced alpha particle spectroscopic factors.

### I. INTRODUCTION

Investigations of the existence of alpha clusters in nuclei have been carried out for a number of years using one of two basic experimental techniques in most cases. First, extensive studies have been carried out using alpha transfer reactions induced by projectiles ranging from  ${}^2\text{H}$  to  ${}^{16}\text{O}$ . These experiments have been analyzed in terms of the distorted-wave Born approximation (DWBA) and have had some success in determining relative alpha spectroscopic factors for various nuclei.<sup>1-4</sup> However, most analyses have had difficulty establishing absolute spectroscopic factors. A second approach is to knock out an alpha particle from the target nucleus. Both proton and alpha projectiles have been used in these studies.<sup>5-8</sup> The knockout data are analyzed in terms of the distorted-wave impulse approximation (DWIA), and are generally more successful in determining absolute spectroscopic factors.<sup>5</sup>

Clearly the two types of experiments complement each other. In transfer reactions large momentum transfers are often involved and therefore these reactions are excellent tools for studying high spin states and probing higher momentum components of the transferred cluster-core wave function, particularly at higher energy. For example, the momentum mismatch in the ( $d, {}^6\text{Li}$ ) reaction at 100 MeV is  $\approx 200$  MeV/c. On the other hand, due to the kinematics of the three-body final state, exact momentum matching is always possible in the ( $p, p\alpha$ ) reaction independent of the bombarding energy. This enables the determination of quantitative information on the low momentum components of the alpha cluster wave func-

tion. Because of distortion effects, the sensitivity to the higher momentum components is reduced when energy sharing data are obtained for quasifree angle pairs (angle pairs for which zero momentum of the recoiling nucleus is possible). This is a consequence of the fact that the momentum range spanned depends upon the division of energy between the emitted proton and alpha particle. For example, in the coplanar  ${}^9\text{Be}(p, p\alpha){}^5\text{He}$  experiment of Ref. 8, the emitted proton energy falls from  $\sim 62$  MeV at zero recoil momentum to  $\sim 32$  MeV at 220 MeV/c. Since these energies are comparable to the strength of the real part of the proton optical potential large refractive effects result which are not offset by the corresponding increase in the emitted alpha particle energy. Thus, distortion effects lead to an average over the various momentum components which is dominated by the abundant low momentum terms. To overcome this insensitivity to the higher momenta, a common practice has been to make measurements at angle pairs away from the quasifree regions. However, this introduces an additional complication in that the two-body  $p$ - $\alpha$  vertex also changes. Thus, this treatment crucially depends on the validity of the factorization approximation and a minimal impact of the off-energy-shell behavior of the two-body cross section.<sup>9</sup> In addition, the distortion effects can depend sensitively on the angles and energies of the outgoing particles.

It therefore seems appropriate to utilize the distinct advantages of the knockout reaction to probe both the low momentum and high momentum components of the cluster wave function, but with a geometry that keeps both the two-body vertex and the distortion effects essentially constant.

To this end we have made measurements of the ( $p, p\alpha$ ) reaction in a non-coplanar geometry. While maintaining the separation between the  $p$  and  $\alpha$  detectors essentially constant, the  $\alpha$  detector was moved out of the reaction plane defined by the incoming and outgoing proton momenta. For each out-of-plane angle the point in the energy sharing spectrum representing the minimum value of recoil momentum of the residual nucleus approximately corresponds to a constant two-body  $t$  matrix as well as constant energies for the outgoing particles (thereby requiring optical model potentials at a single energy only). Data at other points on the energy sharing spectrum for each non-coplanar angle allow further tests of the DWIA treatment.

As an initial test of the improved sensitivity of this geometry to higher momentum components we have chosen the target  $^9\text{Be}$ . The  $^9\text{Be} - ^5\text{He}$  ground state transition has approximately equal contribution from both  $L=0$  and  $L=2$  knockout according to the shell model calculations.<sup>9</sup> Thus, measurements of higher momentum components will be dominated by  $L=2$ . In addition, the in-plane angles were chosen so that both the ( $p, p\alpha$ ) and ( $p, d^3\text{He}$ ) reactions could simultaneously be quasifree angle pairs. These data provide further tests of the reaction mechanism.<sup>10</sup>

In Sec. II we describe our experimental procedures. The experimental results are discussed in Sec. III, and DWIA analyses of the data are presented in Sec. IV. Finally, conclusions and implications of our data are given in Sec. V.

## II. EXPERIMENTAL PROCEDURES

The experiment was carried out using the 101.5 MeV proton beam from the University of Maryland Isochronous Cyclotron. After momentum analysis ( $\Delta p/p \approx 0.04\%$ ) the beam was focused at the center of a 1.5 m diameter scattering chamber. The size of the beam spot on target was approximately  $2\text{ mm} \times 2\text{ mm}$  and the energy of the beam was known to 0.5 MeV.

The experimental setup in the scattering chamber is shown in Fig. 1. The proton detector was placed at  $\theta_1 = 81.2^\circ$  in the horizontal (scattering) plane. It consisted of a  $500\ \mu\text{m}$  silicon surface barrier  $\Delta E$  detector followed by a 15 mm thick Hyperpure germanium  $E$  detector. This telescope system subtended a solid angle of 5.2 msr. On the opposite side of the beam a precision out-of-plane device was mounted on a movable arm. For any in-plane angle  $\theta_2$ , the out-of-plane angle,  $\beta$ , can be varied remotely from  $-5^\circ$  to  $+90^\circ$  along a circular arc in a vertical plane centered on the

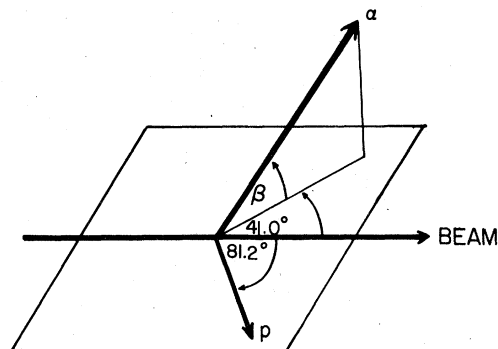


FIG. 1. Experimental configuration for the non-coplanar ( $p, p\alpha$ ) measurement.

target. A vertical plate on this device facilitated the mounting of several detectors at different angles,  $\beta$ . Three alpha detectors separated by  $\sim 10^\circ$  were used for this experiment. Each consisted of a 3 mm lithium-drifted silicon detector and subtended a solid angle of 0.84 msr. The in-plane angle was fixed at  $\theta_2 = -41.0^\circ$ , and data obtained for  $\beta = 0^\circ - 21^\circ$ .

The outputs of all detectors were fed to charge sensitive preamplifiers. The slow linear signals from the proton telescope were used to obtain  $\Delta E - E$  coincidence. The fast signal from the  $\Delta E$  detector was used as a start signal for a time-to-amplitude converter (TAC). The fast outputs from the three alpha detectors provided the stop signal. Thus, real and random coincidences were stored simultaneously.

The amplified linear signals from each detector and the TAC signal, suitably gated by the  $\Delta E - E$  coincidence, were fed to 4096 channel analog-to-digital converters interfaced to an IBM 360/44 computer. Particle identification (PID) for the proton arm was performed by software. No particle identification was required for the alpha detectors, due to the differences in the kinematics of the various possible reactions. One- and two-dimensional histograms of the energy signals were generated. Calculated kinematic loci displayed on the two-dimensional coincidence energy spectra were used to identify the various events. Pulsar signals fed to each preamplifier and analyzed together with the real data were used to correct for electronic dead time losses. On-line visual displays of the various histograms were used to monitor the quality of the PID, gain stability, dead time losses, and statistics for the different coincident events. In addition to this on-line analysis the data were written event by event on magnetic tapes for later, more careful data reduction.

## III. EXPERIMENTAL RESULTS

Energy sharing distributions were obtained for  $(p, p\alpha)$  and  $(p, d^3\text{He})$  at ten out-of-plane angles, ranging from zero to  $21^\circ$ . A plot of the  $(p, p\alpha)$  data as a function of the energy of the outgoing proton is shown in Fig. 2. The detected proton energy ranges from  $\sim 35$  to  $\sim 75$  MeV, the upper limit set by the thickness of the germanium detector. A smooth variation of the cross sections with proton energy is noted, except for the region near 70 MeV, where a broad peak is observed. If we assume that this peak is not due to quasi-free knockout and that, in each energy sharing distribution, the quasifree contribution is symmetric around the minimum recoil momentum and equal in magnitude to the lower proton energy side, there remains a broad peak centered at  $\sim 70$  MeV and having a cross section of about  $5 \mu\text{b}/\text{sr}^2 \text{MeV}$ , independent of the out-of-plane angle. This indicates that the outgoing alpha's

coincident with the 70 MeV protons are isotropic. Kinematic calculations seem to confirm that this peak is consistent with inelastic scattering of protons to the broad state in  $^9\text{Be}$  around 15.4 MeV, followed by alpha decay to the ground state of  $^5\text{He}$ . This type of sequential decay peak has also been observed in other knockout reactions.

For the  $(p, p\alpha)$  triple differential cross sections shown in Fig. 2, the range of the recoil momentum ( $P_3$ ) of the residual nucleus falls with increasing out-of-plane angle. Specifically, the minimum value ranges from zero for the in-plane data to  $190 \text{ MeV}/c$  for  $\beta = 21^\circ$ , whereas the maximum  $P_3$  remains essentially constant. As expected the in-plane data peaks at  $P_3 = 0$  due to the dominance of the  $L = 0$  knockout for low recoil momenta.

In Fig. 3 the cross sections for the minimum recoil momentum (crosses) are superimposed on the in-plane energy sharing data (dots), as a function of  $P_3$ . It is interesting to note that the structure of the out-of-plane data differs significantly

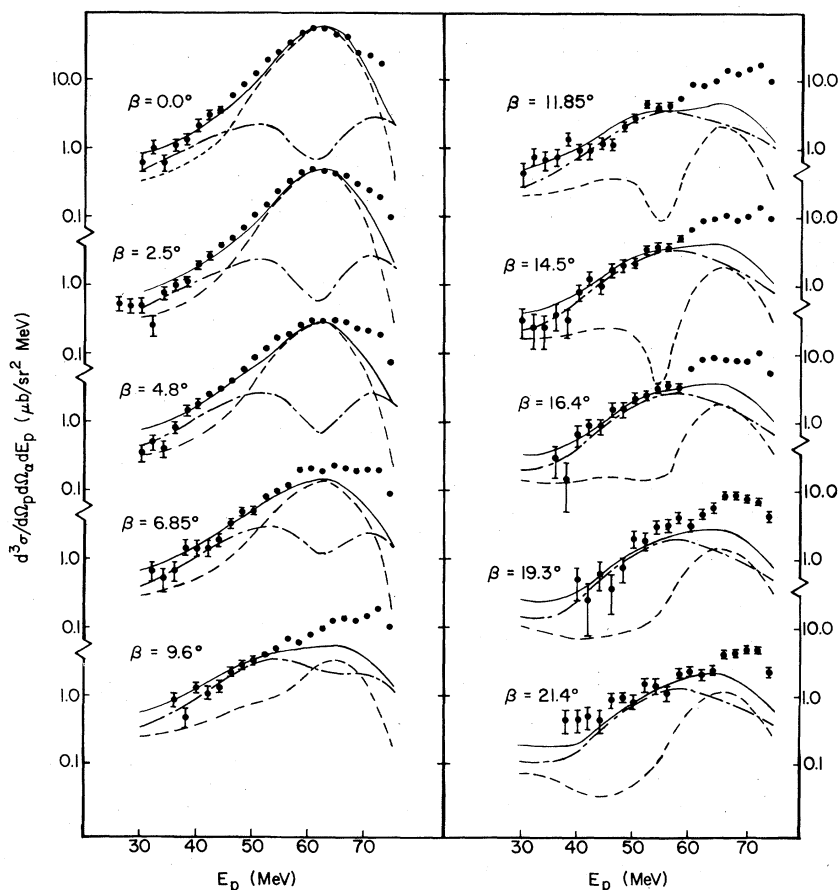


FIG. 2. Energy sharing distributions for the  $^9\text{Be}(p, p\alpha)^5\text{He}$  reaction for out-of-plane angles ranging from  $0^\circ$  to  $21.4^\circ$ . The curves are DWIA calculations discussed in the text.

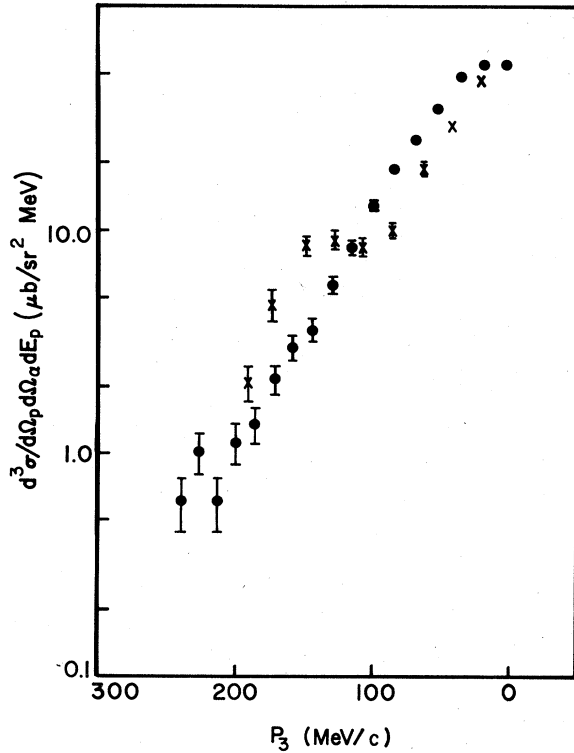


FIG. 3. Cross sections  $d^3\sigma/d\Omega_p d\Omega_\alpha dE_p$  versus recoil momentum ( $P_3$ ) for  ${}^9\text{Be}(p, p\alpha){}^5\text{He}$  at 101.5 MeV. The dots represent the in-plane data and the crosses represent the cross sections taken from the out-of-plane data at the minimum recoil momenta.

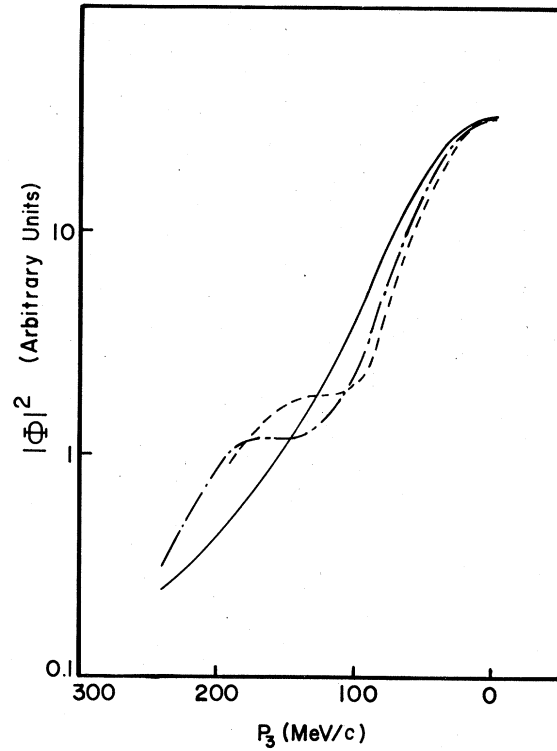


FIG. 4. In-plane distorted (solid line) and undistorted (dot-dash line) momentum distributions as functions of recoil momentum ( $P_3$ ). The dashed line represents calculations for the out-of-plane minimum recoil momentum points.

from the in-plane data. For low momentum transfer the out-of-plane distributions appear narrower. In addition, the out-of-plane data show a prominent peak around  $P_3 = 150$  MeV/c. Both effects are indications of less severe distortion in the out-of-plane data. This interpretation is supported by DWIA calculations. In Fig. 4 the quantity  $\sum_A |T_L^\Lambda|^2$ , where  $T_L^\Lambda$  is the DWIA transition amplitude defined in Sec. IV, is plotted as a function of  $P_3$ . In the limit of no distortions this quantity reduces to  $|\Phi(-\vec{P}_3)|^2$ , where  $\Phi(\vec{q})$  is the struck alpha particle momentum wave function at a momentum  $\vec{q}$ . The in-plane distorted momentum distribution (solid line) shows a smooth variation with  $P_3$ , in agreement with the in-plane data. The undistorted momentum distribution (dot-dashed line) is narrower for low momenta and shows an enhancement around 150–200 MeV/c, due to the  $D$ -state contribution. The dashed line, which represents distorted wave calculations for minimum recoil momenta for various out-of-plane angles, is clearly more similar in shape to the undistorted momentum distribution than are the in-plane distorted wave calculations.

This result is consistent with the assumption that changes in the distortion of the outgoing proton wave function have greater influence on the data than those due to the alpha-particle wave function. For a recoil momentum of 150 MeV/c, the energy of the outgoing proton is about 35 MeV in the in-plane case and 62 MeV in the out-of-plane case. We find that although distortion effects are not negligible at 62 MeV, their severity increases very rapidly as the proton energy is lowered.

The ( $p, d^3\text{He}$ ) energy sharing distributions for the 10 angle pairs are shown in Fig. 5. Again the prominent peak at zero recoil momentum for the in-plane data is indicative of the dominance of  $L=0$  transfer. As the out-of-plane angle increases, one observes a flattening of the distribution due to the increased sensitivity to the  $D$ -state contribution. The structure of the minimum recoil momentum out-of-plane data is very similar to that of the ( $p, p\alpha$ ) data, in spite of the fact that a 2-body reaction now occurs in the upper vertex. This is further confirmation of the hypothesis that distortions are responsible for smear-

ing out the structure in the in-plane data.

Also noticeable in Fig. 5 are large yields in regions above  $E_d = 40$  MeV, which do not appear to result from a quasifree reaction. Nevertheless one cannot rule out the possibility that these enhancements are due to distortion effects, particularly considering the fact that the out-going  ${}^3\text{He}$  energies are less than 30 MeV. Alternatively, they could be interpreted as some sequential process resulting from the breakup of the target nucleus. However, further investigations would be required to explain this large high energy yield.

#### IV. DWIA ANALYSES

Several experimental studies have demonstrated that the impulse approximation is rather well satisfied in the energy region around 100 MeV.<sup>8,11,12</sup> It has also been shown that distortion effects must not be neglected at any energy.<sup>13</sup> Therefore, we have analyzed the data in terms of the distorted-wave impulse approximation

(DWIA). In the DWIA the triple differential cross section for  $(p, p\alpha)$  reactions can be written<sup>13</sup> as

$$d^3\sigma/d\Omega_p d\Omega_\alpha dE_p = S_\alpha F_K \frac{d\sigma}{d\Omega_{p-\alpha}} \sum_\Lambda |T_L^\Lambda|^2, \quad (1)$$

where  $S_\alpha$  is the alpha-cluster spectroscopic factor and  $F_K$  is a known kinematic factor. In the form of Eq. (1), generally referred to as the factorized DWIA, the  $p$ - $\alpha$  interaction has been taken out of the integration in  $T_L^\Lambda$  and evaluated for the asymptotic (final state) kinematics of the  $p$ - $\alpha$  system. The validity of this factorization approximation has been checked<sup>8</sup> and found to be reasonable for the  ${}^9\text{Be}(p, p\alpha)$  reaction. Any uncertainty in the true behavior of this off-energy shell cross section is less of a problem for the out-of-plane data, since the kinematics of the two-body final state is nearly constant.

The quantity

$$T_L^\Lambda = (2L+1)^{-1/2} \int \chi_p^{(-)*}(\vec{r}) \chi_\alpha^{(-)*}(\vec{r}) \phi_L^\Lambda(\vec{r}) \chi_p^+(\gamma\vec{r}) d\vec{r} \quad (2)$$

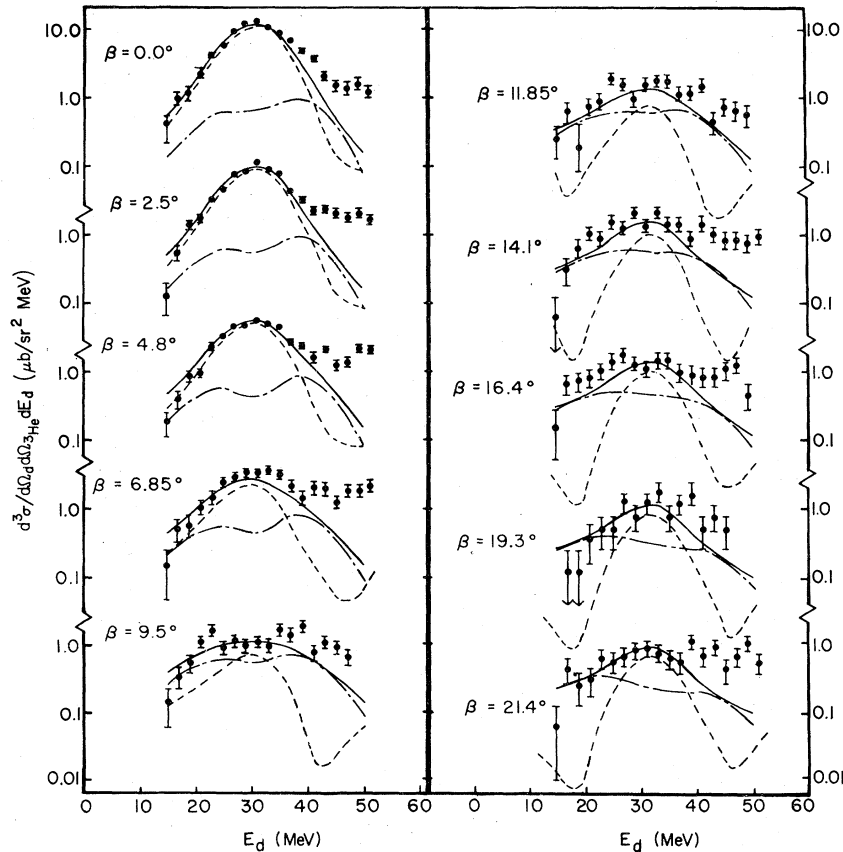


FIG. 5. Energy sharing distributions for the  ${}^9\text{Be}(p, d {}^3\text{He}){}^5\text{He}$  reaction for out-of-plane angles ranging from  $0^\circ$  to  $21.4^\circ$ . The curves are DWIA calculations discussed in the text.

is commonly referred to as the distorted momentum distribution, since in the plane wave limit it reduces to the momentum wave function for the alpha cluster in the target nucleus. The  $\chi$ 's are distorted waves for the incoming proton and the outgoing proton and alpha particles,  $\phi$  is the alpha particle bound state wave function and,  $\gamma=B/A$  is the ratio of residual and target masses.

The DWIA calculations were carried with the code THREEDEE written by Chant.<sup>13</sup> The distorted waves were generated from potential parameters determined by optical model fits to elastic scattering data.

The bound alpha-cluster wave function was replaced by an eigenfunction of a Woods-Saxon potential well with an energy eigenvalue equal to the separation energy of the alpha particle from the target nucleus. The geometry parameters of the well were chosen to approximate folding model calculations<sup>8</sup> which have been reasonably successful in fitting low energy alpha-particle elastic scattering and in predicting bound state properties for  $s$ - $d$  shell nuclei. The principal quantum number of the bound state wave function was chosen on the basis of the conservation of oscillator shell model quanta. Since both the target and ground state of the residual nucleus have total angular momentum and parity  $J^\pi = \frac{3}{2}^-$ , both  $S$  and  $D$  cluster knockouts are possible. Assuming a  $(1s^4)(1p^5)$  configuration for  $^9\text{Be}$  and using the law for conservation of oscillator quanta

$$2(N-1)+L = \sum_{i=1}^4 2(n_i-1)+l_i, \quad (3)$$

we find that  $3S$  and  $2D$  wave functions contribute. Consequently, we carried out  $3S$  and  $2D$  calculations for all the data.

The potential parameters used in the calculations are listed in Table I. For the incoming channel we needed a  $p+^9\text{Be}$  potential at 100 MeV, but no such potential exists. Therefore, we used potentials obtained from  $p+^{12}\text{C}$  elastic scattering at 100 MeV.<sup>14</sup> Since the  $p+\alpha$  interaction is explicitly accounted for in the two-body interaction, the strengths of these potentials were multiplied by  $B/A$  to exclude that part of the interaction. For the  $p+^5\text{He}$  interaction in the outgoing channel,

$p+^6\text{Li}$  potential parameters at 50 MeV were used,<sup>15</sup> while for the  $\alpha+^5\text{He}$  channel, the  $\alpha+^6\text{Li}$  parameters at 30 MeV (Ref. 16) were used. In order to investigate the sensitivity of the DWIA calculations to the distorting potentials, we tried several sets of potentials and found that the shapes of the predicted distributions remained essentially the same and the normalization changed by at most 25%.

Since the in-plane data peak at  $P_3=0$ , they are most sensitive to the  $S$ -state contribution. Therefore, these data were used to determine the  $S$ -state normalization. The value obtained for  $S_\alpha(L=0)$  is 0.45. This normalization for the  $S$ -state contribution was maintained for all the out-of-plane data. Because of the larger momentum transfers involved, the out-of-plane data are more sensitive to the  $D$ -state contributions and are thus found to be very effective in the determination of the  $D$ -state normalization which was found to be 0.55.

The calculations, appropriately normalized, are shown in Fig. 2. The dashed lines represent the normalized  $S$ -state calculations, the dot-dashed lines represent the normalized  $D$ -state calculations, and the solid line represents the incoherent sum of the two. It is gratifying to note that without changing the  $S$ - and  $D$ -state normalization all out-of-plane angles can be reasonably well reproduced, at least on the low energy side of the data where sequential effects are negligible. The fact that we cannot reproduce the peak around 70 MeV seems to confirm the suggestion that it is due to processes not included in the DWIA, such as sequential processes.

For the analysis of the ( $p, d^3\text{He}$ ) data, the same formalism expressed in Eq. (1) was used, except that the proper  $Q$  value was taken into account and the  $p-\alpha$  elastic cross section was replaced by the  $^4\text{He}(p, d)^3\text{He}$  free cross section at the appropriate energies. The same alpha particle bound state parameters as in the ( $p, p\alpha$ ) calculations were used. The distorting potentials for the incident proton were the same as those used for ( $p, p\alpha$ ). For the outgoing deuterons and  $^3\text{He}$  we have adopted the potentials used by Cowley *et al.*<sup>10</sup> The sensitivity of the calculations to other dis-

TABLE I. Optical potential parameters.

System	$V$	$r_0$	$a_0$	$W$	$W_D$	$r_w$	$a_w$	$r_c$	Ref.
$p+^9\text{Be}$	14.22	1.02	0.65	3.7	0	1.70	0.216	1.33	14
$p+^5\text{He}$	37.8	1.14	0.79	0	4.48	1.32	0.48	1.2	15
$\alpha+^5\text{He}$	72.63	1.36	0.765	23.8	0	1.34	0.765	1.3	16
Bound state	89.2	1.35	0.73					1.35	8

torting potentials was negligible. With potentials whose volume integrals differed by a factor of 2 from those used, the shapes of the calculated distributions remained essentially unchanged with the overall normalization changing by no more than 20%. However, when the  $d + ^4\text{He}$  potential of Hinterberger *et al.*<sup>17</sup> was used, the peak of the in-plane distribution was shifted up by 1.5 MeV, inconsistent with other calculations and the data. This might be attributed to the unusually small radius parameters used in their analysis.

The calculations with the same normalization as for the  $(p, p\alpha)$  data (i.e., 0.45 for the  $S$  state and 0.55 for the  $D$  state) are shown in Fig. 5. The dashed lines represent the  $S$  state, the dot-dashed lines represent the  $D$  state, and the solid line represents the incoherent sum of both. It is interesting to note that the spectroscopic factors obtained from both  $(p, p\alpha)$  and  $(p, d\ ^3\text{He})$  are about the same. A slightly better fit could be obtained for the  $(p, d\ ^3\text{He})$  data if the  $S$  state were increased by 10%, but this is well within the limits of the uncertainty in the extracted spectroscopic factor.

#### V. CONCLUSIONS

We have made concurrent measurements of  $(p, p\alpha)$  and  $(p, d\ ^3\text{He})$  on  $^9\text{Be}$  for ten out-of-plane angles ranging from  $0^\circ$  to  $21^\circ$ . In both cases, as the out-of-plane angle is increased, the data vary as expected for a quasifree knockout re-

action in which both  $S$  and  $D$  states contribute.

Comparison of the data with distorted wave calculations clearly indicates that the DWIA treatment of the reaction is viable. The agreement between experiment and calculation for the two different reactions over the large range of non-coplanar angles is remarkable. The shape of the energy sharing distribution is well reproduced in all cases and the same normalization (0.45 for  $S$  and 0.55 for  $D$ ) applies for all angles.

The absolute spectroscopic factors extracted from the data agree well with the theoretical predictions of Kurath, who finds  $S_\alpha(3S) = 0.56$  and  $S_\alpha(2D) = 0.55$ . Our value of 0.45 for the  $S$  state is also in agreement with previous work.<sup>8,10</sup> However, the present work is the first to cleanly separate the  $D$  state from the  $S$  state and to unambiguously determine a value of the spectroscopic factor for the  $D$  state, thereby confirming the validity of the theoretical predictions.

#### ACKNOWLEDGMENTS

We would like to thank the entire cyclotron staff for their efforts in providing us with high quality and stable beams during these studies. We gratefully acknowledge the University of Maryland Computer Science Center for their generous allocation of computer time for the extensive DWIA calculations. This work was supported in part by the National Science Foundation.

\*Present address: P Division, Los Alamos Scientific Laboratory, Los Alamos, New Mexico.

<sup>1</sup>F. D. Becchetti, *Proceedings of the Third International Conference on Clustering Aspects of Nuclear Structure and Nuclear Reactions, Winnipeg, 1978*, edited by W. T. A. van Oers, J. P. Svenne, J. S. C. McKee, and W. R. Falk (AIP, New York, 1978), p. 308, and references therein.

<sup>2</sup>G. J. Wozniak, D. P. Stahel, J. Cerny, and W. A. Jelley, *Phys. Rev. C* **14**, 815 (1976).

<sup>3</sup>N. Anantaraman *et al.*, *Phys. Rev. Lett.* **35**, 1131 (1975).

<sup>4</sup>H. Yoshida, *Phys. Lett.* **47B**, 411 (1973).

<sup>5</sup>N. S. Chant, in *Proceedings of the Third International Conference on Clustering Aspects of Nuclear Structure and Nuclear Reactions, Winnipeg, 1978*, edited by W. T. A. van Oers, J. P. Svenne, J. S. C. McKee, and

W. R. Falk (AIP, New York, 1978), p. 415, and references therein.

<sup>6</sup>J. D. Sherman, D. L. Hendrie, and N. S. Zisman, *Phys. Rev. C* **13**, 20 (1976).

<sup>7</sup>D. Bachelier *et al.*, *Nucl. Phys.* **A268**, 488 (1976).

<sup>8</sup>P. G. Roos *et al.*, *Phys. Rev. C* **15**, 69 (1977).

<sup>9</sup>D. Kurath, *Phys. Rev. C* **7**, 1390 (1973).

<sup>10</sup>A. A. Cowley *et al.*, *Phys. Rev. C* **15**, 1650 (1977).

<sup>11</sup>P. G. Roos *et al.*, *Phys. Rev. Lett.* **40**, 1439 (1978).

<sup>12</sup>C. W. Wang *et al.*, *Phys. Rev. C* **21**, 1705 (1980).

<sup>13</sup>N. S. Chant and P. G. Roos, *Phys. Rev. C* **15**, 57 (1977).

<sup>14</sup>R. M. Haybron, *Nucl. Phys.* **A124**, 662 (1969).

<sup>15</sup>G. S. Mani, D. Jacques, and A. D. B. Dix, *Nucl. Phys.* **A165**, 145 (1971).

<sup>16</sup>S. Matsuki *et al.*, *J. Phys. Soc. Jpn.* **26**, 1344 (1969).

<sup>17</sup>F. Hinterberger *et al.*, *Nucl. Phys.* **A111**, 265 (1968).